International Journal of Advance Research in Science and Engineering
Volume No.06, Special Issue No.(01), December 2017
www.ijarse.com
IJARSE
ISSN: 2319-8354

INVESTIGATION OF THE RADIAL BLOWER FOR TELECOMMUNICATION SYSTEM COOLING USING CFD

K. Vijay Kumar

Research scholar, Department of Mechanical Engineering, SSSUTMS, BHOPAL, (INDIA)

ABSTRACT

CFD models for fans and radial blowers involve information about blades' geometry, flow angles, blade's rotational speed, and flow approach velocities. Accurate simulations of models require large numbers of mesh points which is beyond the allocated time and available resources for design cycles. When dealing with system or board level thermal analysis, where a fan or a blower is among many components need to be modeled, A "macro "model for a fan is a plane surface that induces pressure across as the flow passes through it. A "macro" model for a radial blower is more involved because of the 90° flow turn inside the blower's housing and induced flow swirl caused by impeller blades. The need to capture the flow turn, induced swirl becomes more evident when simulating multiple interacting blowers inside a blower tray. In this paper, a systematic approach is presented to design the blower macro from the existing fan model. The Icepack CFD results for the blower tray have been analyzed. A typical use of a three fan blower tray in a system representing telecommunication function is also presented at the end.

Keywords: Blower, CFD, Flow angles, pressure, Thermal analysis.

I.INTRODUCTION

Axial flow fan is extensively used in many engineering applications. Its adaptability has resulted in implementation into large scale systems, from industrial dryers and air conditioning units to automotive engine cooling and in-cabin air recirculation systems. The benefit of using axial flow fans for the purpose of augmenting heat transfer is particularly evident in the automobile industry because of the need for relatively compact designs. The extended use of axial flow fans for fluid movement and heat transfer has resulted in detailed research into the performance attributes of many designs. Numerical investigations have been performed to quantify the performance of axial fans and their flow characteristics. However, the more-practical example of cooling a heated engine or heated plate using an axial flow fan has received more attention in regards to understanding flow characteristics and heat transfer. With the expressive computer capability and extensive development in the simulation field, CFD have drawn attention in recent years.

International Journal of Advance Research in Science and Engineering
Volume No.06, Special Issue No.(01), December 2017
www.ijarse.com
IJARSE
ISSN: 2319-8354

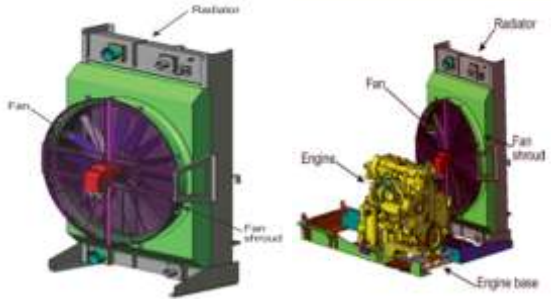

Fig. 1 Radiator fan assembly & Cooling System

1.1 PROBLEM STATEMENT AND OBJECTIVE

The efficiency of automotive radiator is largely dependent on the ability of the fan to force the air draught as much as possible. In order to devise an effective fan design, the primary objective is to maintain desired pressure difference between the fan inlet and outlet. The radiator fan design was first evaluated through simulations to obtain pressure difference and torque values. In order to obtain the desired pressure difference and torque. The radiator fan with 12 blades was first analyzed through CFD simulations and the pressure difference between the fan inlet and outlet were measured. To improve performance keeping the same number of blade and discharge with changing the rotational speed of the fan were suggested and flow analysis for the same was performed. Desired pressure difference was obtained through the various rotational speeds. Final results show better efficiency calculating by the numerical simulation. This solution can also be provided using FLUENT.

II.DESIGN AND CFD ANALYSIS OF RADIATOR FAN ASSEMBLY

2.1 DESIGN

The first step is to identify a typical radiator axial flow fan that can be reproduced as a 3-D CAD Solid works software engineering drawing package (Fig. 2). The 3-D models are then imported into the CFD software, remodeled into different sections, and refined to generate a finite volume meshing (Fig. 3). This is a crucial step, where details of the geometrical shape need to be defined precisely. The flow domain is also created, and the final meshing of all components needs to be accurate. The total element count will be around 1.6 million, with an inflation layer on the blades. Any errors in the drawings and flow area need to be corrected before continuing.

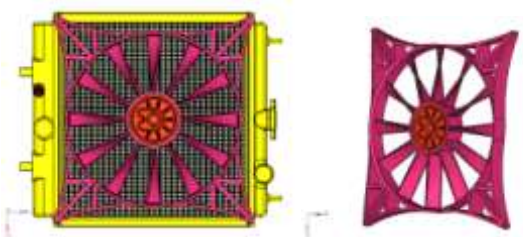

Fig. 2 Computational domain of a fan

The second step is to import the files into the CFD code preprocessor, which will solve the flow equations. Here, the flow fields boundary conditions are set. These include inlet air mass flow, outlet pressure, fluid

properties, and flow domain characterization, such as moving internal zone and stationary solid walls. The next step is to set the simulation process as a 3-D steady and turbulent problem.

Table 1 FAN-SHROUD Assembly Specifications

Specification	
Number of Blades	12
Fan Diameter	300 mm
Blade Thickness	4.25mm
Height of the blade	100mm
Hub outer diameter	100mm
Hub Thickness	37mm
Rotation	CW from Front End

FAN-Geometry and Domains

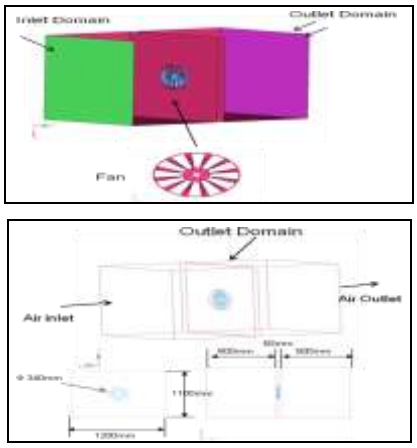

Fig. 3 FAN-Geometry and Domains

Problem setup AND Boundary Conditions

For the steady RANS simulations, the single equation Spalart-Allmaras (SA) turbulence model was used. The turbulence equation is solved segregated from the flow equations using the GLS formulation. Reference Frame is used to simulate the Rotating Flow.The outlet has been modeled with static pressure of 1 atm. Spalart-Allmaras (SA) Turbulence model was used. High Resolution Option was employed for all transport equations. The convergence criteria were a normalized RMS residual on all variables of 1.0e-4, and a 'Conservation target' (i.e. global balance) of 1.0e-3. In convergence controls auto time scaling was employed with conservative length scale option. Type of flow is Steady-state and Incompressible, all wall modeled as adiabatic wall (No Heat Transfer) with no slip condition.

International Journal of Advance Research in Science and Engineering
Volume No.06, Special Issue No.(01), December 2017
www.ijarse.com
IJARSE
ISSN: 2319-8354

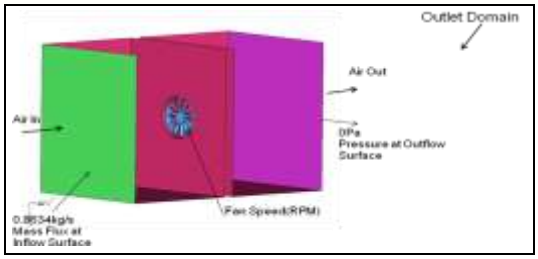

Inlet – Mass Flow inlet, Outlet – Pressure Outlet

Fan –Reference Frame

All other surfaces are No-Slip wall BC

Boundary conditions summary

S. No	Inlet:(Mass flow rate(kg/s)	Outlet:(Pressure (Pa)	RPM
case1	0.8634	**0**	**2700**
case2	0.8634	**0**	**3000**
case3	0.8634	**0**	**3300**
case4	0.8634	**0**	**3600**

2.2 MESHED MODEL-1AND 2

Once the geometry has been the defined, the fluid region of the domain is then filled with elements, forming a computational mesh. The relevant equations are then solved at the vertices (or corners) of these elements, yielding velocities, pressures, temperatures, concentrations, etc. In this case the tetrahedral element type (four triangular faces, four vertices) is used. Hyper mesh 12.0 was used for Meshing. In this case the complete mesh consisted of ~1 million tetrahedral volume elements with 10 layer of the boundary layer. The size of this computational mesh is sufficient to adequately resolve the features of importance. Surface mesh for various parts and vertical section through volume mesh are shown in the following Figures.

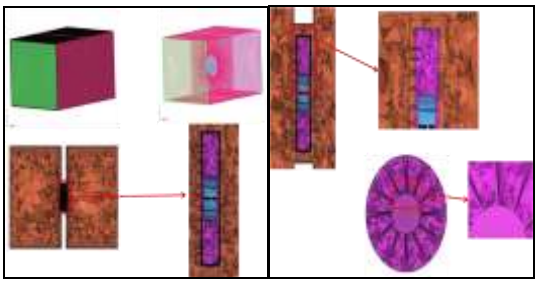

Total number of cells ~954261

Total number of boundary layers--10

International Journal of Advance Research in Science and Engineering
Volume No.06, Special Issue No.(01), December 2017
www.ijarse.com
IJARSE
ISSN: 2319-8354

III. RESULTS AND DISCUSSIONS

On Post processing the numerical CFD results, the observations are presented as velocity vector distributions, flow lines and static pressure contour plot at mid section of the fan and also on rotor. For the velocity vector representation, a plane is taken normal to the y-axis coordinate and at the centre (0, 0, 0,). Results are compiled separately for the front and back oriented blades.

3.1 Analysis results for Case-1, 2700 RPM

Fig. 4.1a, illustrates the velocity magnitude on the rotor, which confirms that velocity increased moving from the hub to the tip on the rotor and thus validated the theoretical concept of V= r.ω. This also affirms that the rotor was rotating at the center point of the fan axis.maximum tip velocity is 40.53m/s.

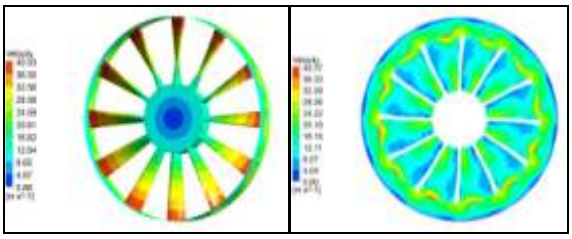

Fig. 4.1a Velocity magnitude on rotor

Fig. 4.1b show the velocity vector distribution, at a plane normal to the y-axis(mid of the rotor). A high flow region formed around the outer diameter of the flow domain and a low reverse flow region formed in the center Fig. 4.1b Velocity magnitude at mid plan of the rotor behind the fan hub. Between the high and low reverse flow regions, there existed strong circulation vortices. Strong circulation regions were also observed behind the fan blades. This helps in understanding the flow behavior around the rotor.

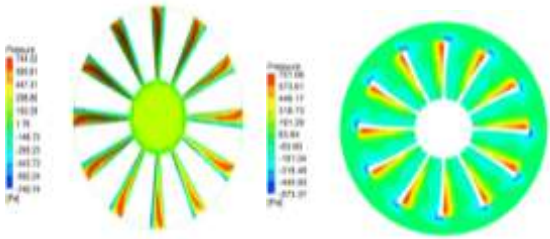

Fig. 4.1c Static pressure on rotor

4.1 d Static pressure at mid plan of the rotor

Figs. 4.1c and 4.1d, show the pressure contours for static pressure at mid plane of the rotor and on rotor. By observing the pressure contour at the rotor,pressure varies from -740.74 pa to 744.32Pa.

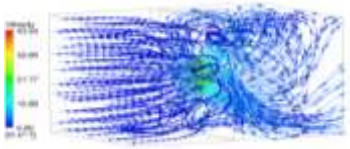

Fig. 4.1e Stream line

Fig.4.1e show the velocity distribution of streamlines from inlet to outlet of the domain. Again, a high flow region formed around the outer diameter of the flow domain (i.e., at the tip side of the blade). Also, a low

reverse flow region formed in the center behind the fan hub. There existed strong circulation vortices in between the high and low reverse flow regions.

3.2 Analysis results for Case-2, 3000 RPM

Fig. 5.1a, illustrates the velocity magnitude on the rotor, which confirms that velocity increased moving from the hub to the tip on the rotor and thus validated the theoretical concept of V= r.ω. This also affirms that the rotor was rotating at the center point of the fan axis.maximum tip velocity is 45.04m/s.

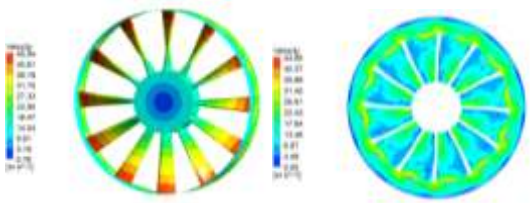

Fig. 5.1a Velocity magnitude on rotor

5.1b Velocity magnitude at mid plan of the rotor

Figs. 5.1b show the velocity vector distribution, at a plane normal to the y-axis(mid of the rotor). A high flow region formed around the outer diameter of the flow domain and a low reverse flow region formed in the center behind the fan hub. Between the high and low reverse flow regions, there existed strong circulation vortices. Strong circulation regions were also observed behind the fan blades. This helps in understanding the flow behavior around the rotor.

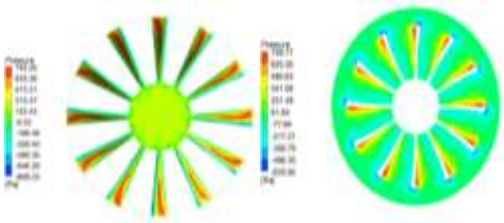

Fig. 5.1c Static pressure on rotor

Fig. 5.1d Static pressure at mid plan of the rotor

Figs. 5.1c and 5.1d, show the pressure contours for static pressure at mid plane of the rotor and on rotor. By observing the pressure contour at the rotor,pressure varies from -806.23 pa to 793.2Pa.

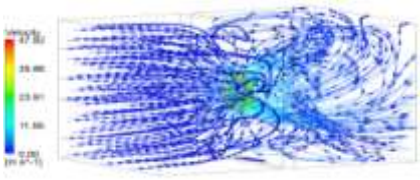

Fig. 5.1e Stream line

Fig.5.1e show the velocity distribution of streamlines from inlet to outlet of the domain. Again, a high flow region formed around the outer diameter of the flow domain (i.e., at the tip side of the blade). Also, a low reverse flow region formed in the center behind the fan hub. There existed strong circulation vortices in between the high and low reverse flow regions.

International Journal of Advance Research in Science and Engineering
Volume No.06, Special Issue No.(01), December 2017
www.ijarse.com
IJARSE
ISSN: 2319-8354

3.3 Analysis results for Case-3, 3300 RPM

Fig. 6.1a, illustrates the velocity magnitude on the rotor, which confirms that velocity increased moving from the hub to the tip on the rotor and thus validated the theoretical concept of V= r.ω. This also affirms that the rotor was rotating at the center point of the fan axis.maximum tip velocity is 49.54m/s.

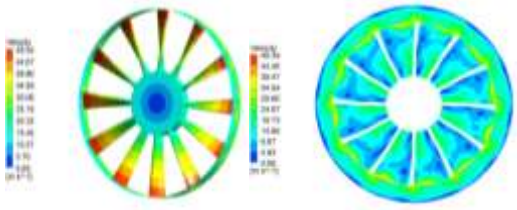

Fig. 6.1a Velocity magnitude on rotor

Fig. 6.1b Velocity magnitude at mid plan of the rotor

Figs. 6.1b show the velocity vector distribution, at a plane normal to the y-axis(mid of the rotor). A high flow region formed around the outer diameter of the flow domain and a low reverse flow region formed in the centerbehind the fan hub. Between the high and low reverse flow regions, there existed strong circulation vortices. Strong circulation regions were also observed behind the fan blades. This helps in understanding the flow behavior around the rotor.

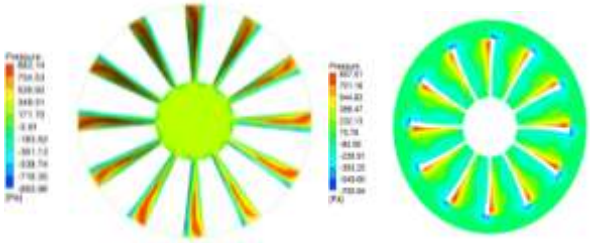

Fig. 6.1c Static pressure on rotor

Fig. 6.1d Static pressure at mid plan of the rotor

Figs. 6.1c and 6.1d, show the pressure contours for static pressure at mid plane of the rotor and on rotor. By observing the pressure contour at the rotor,pressure varies from -893.96 pa to 882.14Pa.

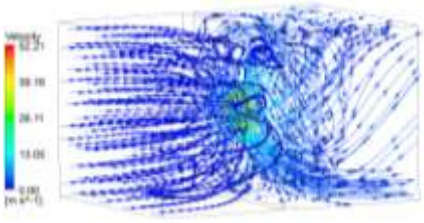

Fig. 6.1e Stream line

Fig.6.1e show the velocity distribution of streamlines from inlet to outlet of the domain. Again, a high flow region formed around the outer diameter of the flow domain (i.e., at the tip side of the blade). Also, a low reverse flow region formed in the center behind the fan hub. There existed strong circulation vortices in between the high and low reverse flow regions.

3.4 Analysis results for Case-4, 3600 RPM

Fig. 7.1a, illustrates the velocity magnitude on the rotor, which confirms that velocity increased moving from the hub to the tip on the rotor and thus validated the theoretical concept of V= r.ω. This also affirms that the rotor was rotating at the center point of the fan axis.maximum tip velocity is 54.04m/s.

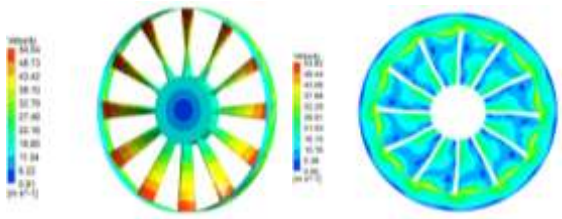

Fig. 7.1a Velocity magnitude on rotor

Fig. 7.1b Velocity magnitude at mid plan of the rotor

Figs. 7.1b show the velocity vector distribution, at a plane normal to the y-axis(mid of the rotor). A high flow region formed around the outer diameter of the flow domain and a low reverse flow region formed in the center behind the fan hub. Between the high and low reverse flow regions, there existed strong circulation vortices. Strong circulation regions were also observed behind the fan blades. This helps in understanding the flow behavior around the rotor.

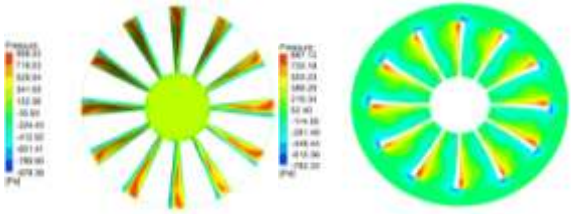

Fig. 7.1c Static pressure on rotor

Fig. 7.1d Static pressure at mid plan of the rotor

Figs. 7.1c and 7.1d, show the pressure contours for static pressure at mid plane of the rotor and on rotor. By observing the pressure contour at the rotor,pressure varies from -978.39 pa to 906.53Pa.

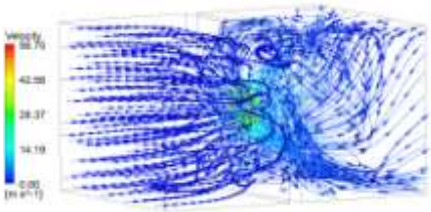

Fig. 7.1e Stream line

Fig.7.1e show the velocity distribution of streamlines from inlet to outlet of the domain. Again, a high flow region formed around the outer diameter of the flow domain (i.e., at the tip side of the blade). Also, a low reverse flow region formed in the center behind the fan hub. There existed strong circulation vortices in between the high and low reverse flow regions.

Pressure losses are calculated for different load cases and are presented below.

Pressure drop for the load cases

S. No	Mass flow rate(kg/s)	Blade speed(RPM)	Delta Pressure(Pa)
Case1	0.8634	2700	163.215
Case2	0.8634	3000	168.356
Case3	0.8634	3300	195.055
Case4	0.8634	3600	189.072

IV.CONCLUSIONS AND SCOPE FOR FUTURE WORK

The results from the numerical simulations provided an insightful understanding of the behavior of fluid flow around the different fan blade speeds. Numerical CFD analysis was performed for a fan with a 2700,3000,3300and 3600 RPM blade speeds. The numerical CFD results were then compared btween the various speeds. The key and important outcomes of this study are as follows

❖ In this work numerical simulation was performed for radiator fan. CFD results to study flow distribution and back pressure estimate. Velocity magnitude, pressure contours & steam line shows flow characteristics that help to understand and verify the main vortex structures found by CFD. Based on this simulation the following conclusions were reached. Radiator fan best operating speed was 3300rpm.

❖ The CFD modeling shown in this study proved to be very helpful in initiating further and more comprehensive numerical study of the off-road engine cooling system.

❖ CFD results were presented in the form of velocity contours and stream lines, which provided actual flow characteristics of air around the fan for different blade orientations.

REFERENCES

[1] Hwa-Ming Nieh, Tun-Ping Teng, Chao-Chieh Yu *"Enhanced heat dissipation of a radiator using oxide nano-coolant"*. International Journal of Thermal Sciences *77, 252-261,* 2013-2014.

[2] M.Naraki and S.M. Peyghambarzadeh, *"Parametric study of overall heat transfer coefficient of CuO/water Nano fluids in a car radiator"*. International Journal of Thermal Sciences *66, 82-90,* 2013.

[3] RahulTarodiya, J. Sarkar, J. V. Tirkey*, "Performance of flat fin tube automotive radiator using Nano fluids as coolants"*. National Conference on Emerging Trends in Mechanical Engineering ETME – 2012.

[4] S.M. Peyghambarzadeh, S.H. Hashemabadi, M. Naraki, Y. Vermahmoudi,*" Experimental study of overall heat transfer coefficient in the application of dilute Nano fluids in the car radiator".*Applied Thermal Engineering *52, 8-16,* 2013.

[5] D. Madhesh, R. Parameshwaran, S. Kalaiselvam,*" Experimental investigation on convective heat transfer and rheological characteristics of Cu–TiO2 hybrid nanofluids".*Experimental Thermal and Fluid Science *52, 104–115,* 2014.

[6] L. Syam Sundar, Manoj K. Singh, Igor Bidkin, Antonio C.M. Sousa, *" Experimental investigations in heat transfer and friction factor of magnetic Ni Nano fluid flowing in a tube"*. International Journal of Heat and Mass Transfer *70, 224–234,* 2014.

[7] Changhua Lin , Jeffrey Saunders , Simon Watkins, *" The Effect of Changes in Ambient and Coolant Radiator Inlet Temperatures and Coolant Flow rate on Specific Dissipation"*. SAE Technical Paper Series, *01-0579, 2000.0879,*2014.

[8] M.M. Elias, I.M. Mahbubul, R. Saidur, M.R. Sohel, I.M. Shahrul, S.S. Khaleduzzaman, S. Sadeghipour, *" Experimental investigation on the thermo-physical properties of Al2O3.nanoparticles suspended in car radiator coolant"*. International Communications in Heat and Mass Transfer *54, 48–53*, 2014.

[9] Adnan M. Hussein, R.A. Bakar, K. Kadirgama, K.V. Sharma, *" Heat transfer enhancement using Nano fluids in an automotive cooling system"*. International Communications in Heat and Mass Transfer *53, 195–202*, 2014.

[10] Adnan M. Hussein, R.A.Bakar, K.Kadirgama, *"Study of forced convection Nano fluid heat transfer in the automotive cooling system"*. Case Studies in Thermal Engineering *50–61*, 2014.

[11] *ANSYS.ANSYS CFX-Solver Theory Guide* 14th edition, ANSYS Inc., 2015.